

AN EXPERIMENTAL STUDY ON EFFECTS OF CORNER-ANCHORED EXTERNAL LATERAL REINFORCEMENT FOR SEISMIC RETROFITTING

(Translation from Proceedings of JSCE, No.676/V-51, May 2001)



Takeshi TSUYOSHI



Tadayoshi ISHIBASHI

Seismic retrofitting of existing RC columns has been in progress in Japan, with steel jacket methods being the most commonly adopted. However, such methods are not applicable where space under RC viaducts is in use by stores and offices. The authors have developed a new seismic retrofitting method which is easily implemented in these cases. In this paper, it is proved that this new method of external lateral reinforcement does not suffer yielding when a gap is left between the reinforcement and the column surface or when the shear-to-flexural-capacity ratio (V_yd/V_{mu}) is over 2.3. It is also proved that, using this new method, equivalent or better flexural capacity can be obtained with less lateral reinforcement compared to RC columns with normal hoop reinforcement.

Key Words: seismic retrofitting method, reinforced concrete column, hoop reinforcement, external lateral reinforcement, ductility

Takeshi Tsuyoshi is a group leader in the Tokaido Sobu Department at the Tokyo Construction Office of East Japan Railway Company. He obtained his D.Eng from the University of Tokyo in 2001. His research interests relate to the seismic design of concrete structures for railways. He is a member of the JSCE.

Tadayoshi Ishibashi is a manager in the Structural Engineering Center of the Construction Department of East Japan Railway Company. He obtained his D.Eng from the University of Tokyo in 1983. His research interests relate to the seismic design of concrete structures for railways. He is a fellow member of the JSCE.

1. Introduction

After the Hanshin-Awaji Earthquake Disaster of Jan.17, 1995, the authorities at the Ministry of Transportation issued a notification to the railway companies relating to seismic retrofitting. Following the recommendations of this notification, seismic retrofitting of the columns of reinforced concrete rigid-frame structures that have a shear-to-moment capacity ratio of below 1.0 has been in progress. Steel jacket methods have typically been used for this purpose. Within the service area of East Japan Railway Company, about ten thousand columns have been retrofitted at present along the Shinkansen Lines and conventional lines in the Minami-Kanto Area and Sendai Area.

The space under railway viaducts is often used in some way, such as by stores and offices, especially in urban areas. This can make it very difficult for large construction machines like cranes, which are used when implementing steel jacket methods, to gain access. In such cases, considerable extra work is entailed in removing these obstacles and compensation must be paid to the stores and offices concerned. As a result, seismic retrofitting is rarely carried out in such cases.

To overcome this problem, we have developed a new seismic retrofitting method which can be executed without machinery and is easily implemented on existing RC columns in confined spaces. **Figure 1** shows an outline of the new method. External lateral reinforcing steel is arranged around an existing RC column and anchored at the four corners with L-section steel. **Figure 2** shows the effect of this seismic retrofitting method [1]. When the shear-to-flexural capacity ratio (V_{yd}/V_{mu} , where V_{yd} : ultimate shear strength after retrofitting; V_{mu} : shear force when the sectional force at the bottom reaches the ultimate flexural strength) reaches 1.4 or more after retrofitting, the ductility ratio (μ) of the RC column exceeds 10. This method has already been executed for the seismic retrofitting of railway structures [2].

The main characteristic of this method is that the retrofitted lateral bars are attached outside the section. In this paper, we report on experimental studies into the differences between hoop reinforcement inside the section and these external retrofitted lateral bars.

2. Experimental Procedure

2.1 Specimens

Table 1 shows the properties of the retrofitted columns and ordinary RC columns used as experimental specimens. In this paper, the ratio of the axial reinforcements are 3.18 to 3.98 %, and the ratio of the shear reinforcements (external lateral reinforcing bars or hoop reinforcements) are 0.32 to 1.07 %, and axial

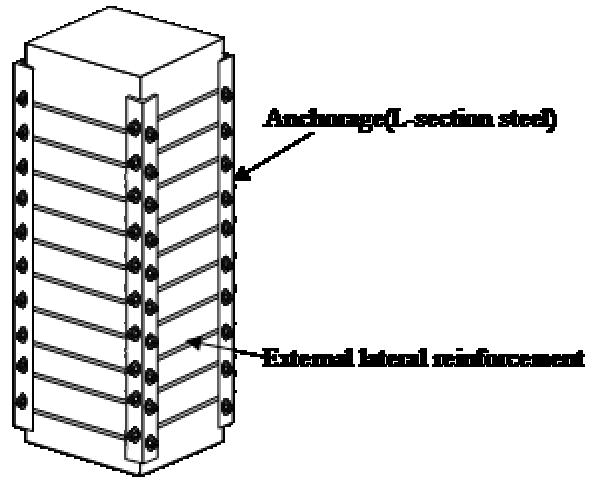


Figure 1 Outline of new seismic retrofitting method

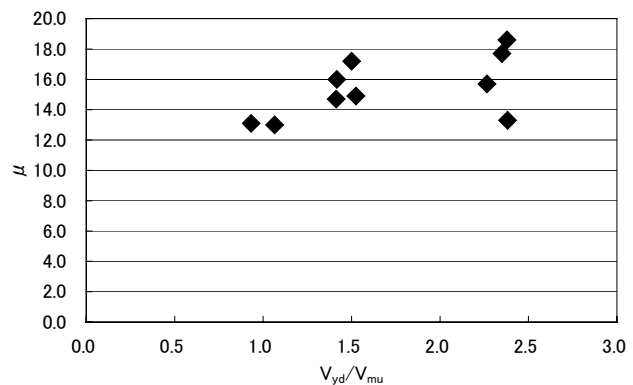


Figure 2 Effect of new seismic retrofitting method[1]

Table 1 Properties of all retrofitted column specimens and ordinary RC column specimens

Specimen number		Section (mm × mm)	Width b (mm)	Effective depth d (mm)	Shear span a (mm)	a/d	Arrangement of axial reinforcement (number)	Ratio of axial reinforcement $A_s/(b \cdot d)$ (%)	Arrangement of lateral external reinforcement (mm)	Ratio of lateral external reinforcement $A_w/(b \cdot s)$ (%)	Axial compressive stress (N/mm ²)	Details of Anchorage		
												Shape of anchorage	L1 (mm)	L2 (mm)
S. R. S.	RB-III-1	400 × 400	400	360	1150	3.19	D19 × 16	3.18	D13@65	0.98	0.98	TypeA	40	25
	RB-III-2	400 × 400	400	360	1150	3.19	D19 × 16	3.18	D13@150	0.42	0.98	TypeA	40	25
	RB-III-3	400 × 400	400	360	1150	3.19	D19 × 20	3.98	D13@200	0.32	0.98	TypeC	40	—
	RB-IV-1	400 × 400	400	360	1150	3.19	D19 × 16	3.18	D13@150	0.42	0.98	TypeB	40	—
	RB-IV-2	400 × 400	400	360	1150	3.19	D19 × 20	3.98	D13@200	0.32	0.98	TypeB	40	—
	RB-V-3	400 × 400	400	360	1150	3.19	D19 × 16	3.18	D13@150	0.42	0.98	TypeD	40	—
	RB-VI-1	600 × 600	600	550	1650	3.00	D25 × 24	3.69	D22@200	0.65	0.98	TypeC	60	—
	RB-VI-2	600 × 600	600	550	1650	3.00	D25 × 24	3.69	D29@200	1.07	0.98	TypeC	60	—
R. C. S.	RC-A1	400 × 400	400	360	1150	3.19	D19 × 16	3.18	D13@80	0.79	0.98	—		
	RC-A2	400 × 400	400	360	1150	3.19	D19 × 16	3.18	D13@60	1.06	0.98	—		
	RC-A4	400 × 400	400	360	1150	3.19	D13 × 16	1.41	D13@80	0.79	0.98	—		
	RC-A5	400 × 400	400	360	1150	3.19	D13 × 16	1.41	D13@140	0.45	0.98	—		
	RC-A6	400 × 400	400	360	1150	3.19	D19 × 16	3.18	D13@50	1.27	0.98	—		
	RC-A8	400 × 400	400	360	1150	3.19	D16 × 16	2.21	D13@120	0.53	0.98	—		
	RC-A9	400 × 400	400	360	1150	3.19	D19 × 16	3.18	D13@60	1.66	0.98	—		
	RC-A11	500 × 500	500	460	1150	2.50	D19 × 16	1.99	D13@60	0.85	0.98	—		
	RC-No. 6	400 × 400	400	360	1150	3.19	D19 × 16	3.18	D13@60	1.06	0.98	—		

S. R. S. : Seismic retrofitted specimens; R. C. S. : Reinforced concrete specimens

Table 2 Material strengths and experimental values

Specimen number		Material strengths							Calculated values			Experimental values	
		Column concrete	Foot-ing concrete	Ancho- rage mortar	Yield strength of axial reinforcement	strength of lateral reinforcement	Yield strain of axial reinforcement	Yield strain of lateral reinforcement	V_c/V_{mu}	V_s/V_{mu}	V_{yd}/V_{mu}	Ductility ratio μ	Failure type
S. R. S.	RB-III-1	20.1	20.7	47.6	377.2	354.6	2072	1931	0.62	1.76	2.38	13.3	F
	RB-III-2	35.7	35.7	61.9	382.8	371.7	2092	2018	0.68	0.73	1.42	16.0	F
	RB-III-3	32.5	32.5	25.8	382.8	371.7	2092	2018	0.60	0.46	1.06	13.0	F.S.
	RB-IV-1	32.5	32.5	55.5	382.8	371.7	2092	2018	0.67	0.74	1.41	14.7	F
	RB-IV-2	31.8	31.8	45.3	382.8	371.7	2092	2018	0.47	0.47	0.93	13.1	F.S.
	RB-V-3	43.2	43.2	40.5	378.5	395.7	1981	2012	0.73	0.77	1.50	17.2	F
	RB-VI-1	27.6	27.6	51.3	368.0	368.2	2006	1981	0.54	0.99	1.52	14.9	F
RB-VI-2	33.0	33.0	53.9	368.0	391.9	2006	2108	0.56	1.71	2.27	15.7	F	
R. C. S.	RC-A1	26.4	31.4	-	378.4	358.3	2069	1980	0.65	1.39	2.05	10.5	F
	RC-A2	23.3	29.0	-	378.4	358.3	2069	1980	0.64	1.89	2.52	12.4	F
	RC-A4	28.4	27.5	-	358.3	358.3	1980	1980	1.09	2.78	3.86	20.6	F
	RC-A5	29.1	29.4	-	358.3	358.3	1980	1980	1.08	1.58	2.66	14.8	F
	RC-A6	31.0	28.6	-	378.4	358.3	2069	1980	0.68	2.20	2.87	15.2	F
	RC-A8	23.8	30.0	-	397.2	358.3	2156	1980	0.75	1.23	1.98	12.1	F
	RC-A9	21.7	22.1	-	378.4	397.2	2069	2156	0.63	3.31	3.94	14.5	F
	RC-A11	24.6	24.4	-	378.4	358.3	2069	1980	0.66	1.70	2.36	13.7	F
	RC-No. 6	19.4	19.6	-	375.1	354.6	2061	1931	0.62	1.94	2.56	13.8	F

S. R. S. : Seismic retrofitted specimens; R. C. S. : Reinforced concrete specimens

F: flexural failure; F.S.: shear failure after flexural yield

compressive stress is 0.98 (N/mm²) and then the ratio of shear span to effective depth is about 3.0.

Figure 3 shows the vertical and horizontal sections of these specimens. **Figure 4** gives details of the anchorages for the external lateral reinforcement. In specimens RB-III-1, -2, and -3, the L-section anchoring steel is continuous in the axial direction, and lateral reinforcing bars are in contact with the surface of the column. The three specimens have different external retrofitting bar ratios. In RB-V-3, separate anchorages are used for each rung of lateral reinforcement in the axial direction, and the space between external lateral

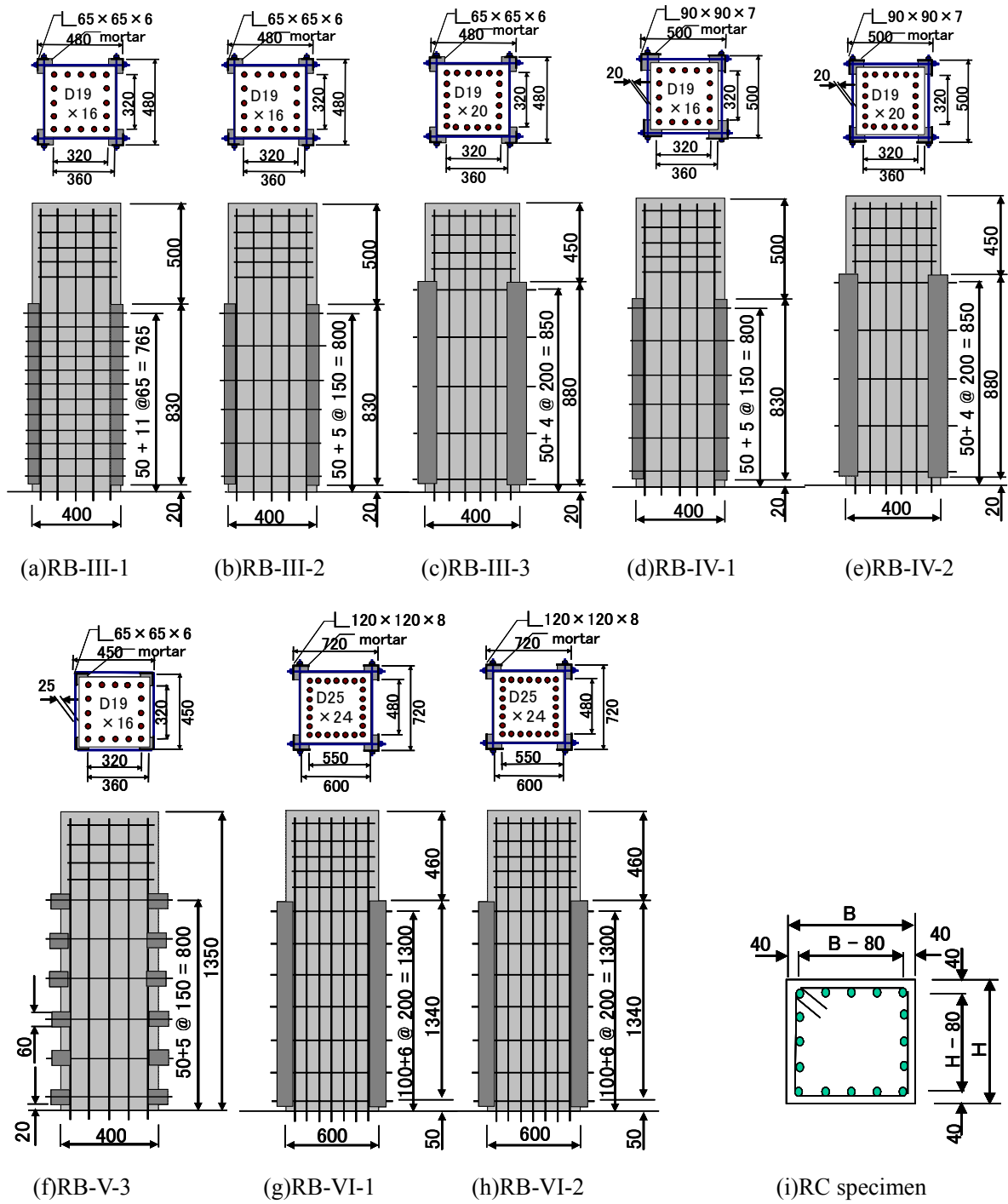


Figure 3 Vertical and horizontal sections of all specimens

reinforcement and there is a 20 mm gap between the reinforcement and the column. Specimens RB-VI-1 and -2 have larger sections than the others and have different retrofitted bar ratios. In these specimens, the L-section anchoring steel is continuous in the axial direction and the lateral reinforcing bars touch the surface of the column. These specimens are chosen such that the experimental parameters are the anchorage arrangement and the gap between retrofitted bars and the surface of the column, which represent levels of efficiency in the actual work.

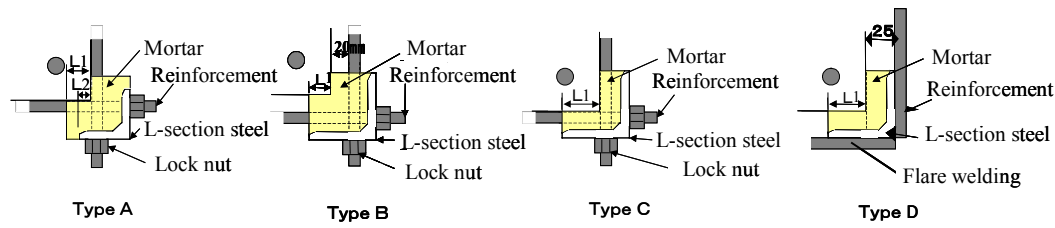


Figure 4 Details of anchorages

The standard specimen characteristics in this experiment are a section of 400(mm) × 400(mm), a ratio of shear span to effective depth of 3.19, and an axial compressive stress of 0.98(N/mm²). These experimental parameters were decided in consideration of actual columns in railway structures.

Table 2 shows the strengths of the materials used and the calculated values of shear-to-flexural capacity ratio. Here, V_c is the ultimate shear strength without shear reinforcement, and V_s is the contribution to ultimate shear strength of the retrofitted bars or the hoop reinforcement. These values are calculated based on the standard specifications for the design of concrete structures for railways [4]. Values of V_s for retrofitted specimens are calculated using truss theory in the same way as for ordinary RC specimens.

2.2 Loading systems

Figure 5 shows the loading systems. All specimens were tested under a constant axial load, and reverse static cyclic loading was applied. The standard yield deformation of each specimen (δ_{ytest}) is defined as the experimental deformation at which the reinforcement which has the largest effective depth reaches yield. Loading was carried out up to δ_{ytest} under load control. Thereafter, cyclic displacement at an integer multiple of δ_{ytest} (δ_{test} : standard flexural yield deformation) was applied ($2\delta_{ytest}$, $3\delta_{ytest}$, $4\delta_{ytest}$, ...). At each loading displacement, one cycle was applied.

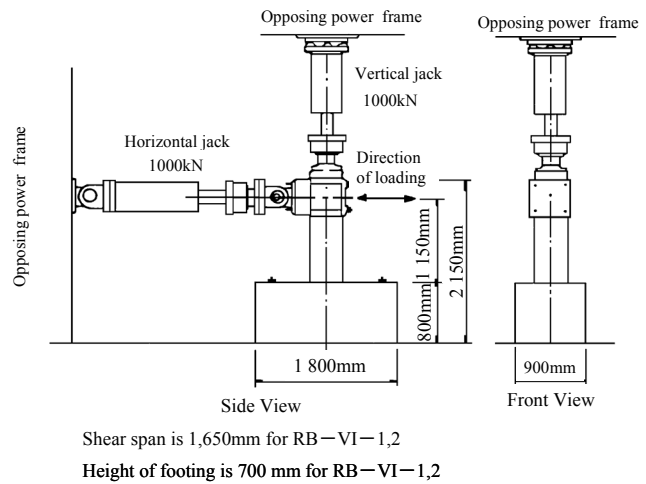


Figure 5 Loading systems

3. Experimental Results and Discussion

3.1 Ductility ratio and failure type

Table 2 shows the experimental results for ductility ratio and type of failure. Ductility ratio is defined as the ratio of experimental ultimate displacement to calculated yield displacement. Here, the experimental ultimate displacement is taken to be the displacement at which the load falls to the yield force. The yield force is the force at which the reinforcement which has the largest effective depth reaches yield, and it is a calculated using the material strengths given in **Table 2**.

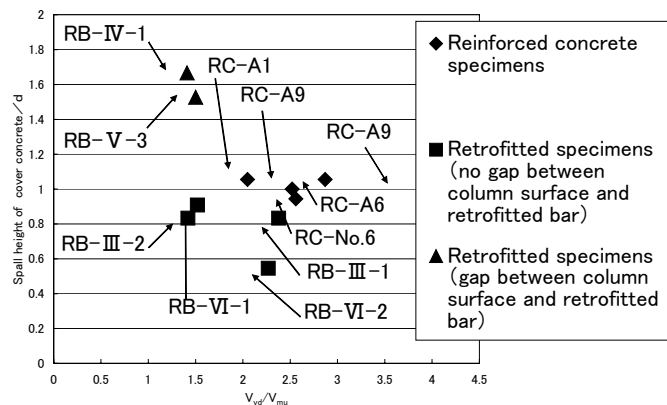


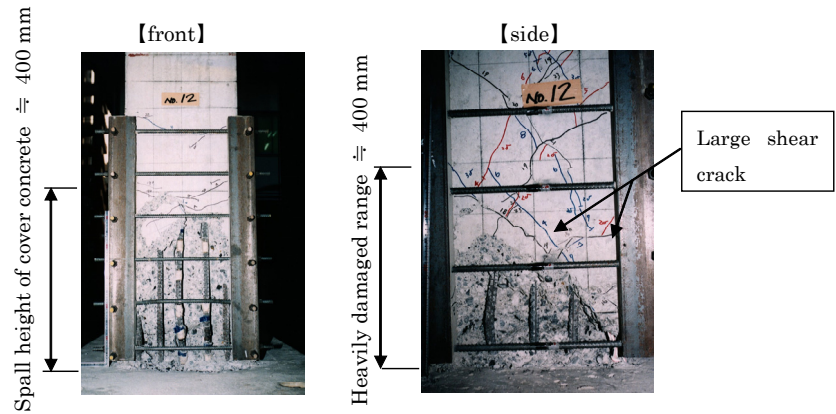
Figure 6 Relationship between height of cover concrete spalling on loaded side and shear-to-flexural capacity ratio

Retrofitted specimens with a shear-to-flexural capacity ratio of more than 1.4 failed in flexure. All RC specimens failed in flexure.

3.2 Loss of cover concrete

In order to compare the damage condition of retrofitted specimens with that of ordinary RC specimens, we studied the area over which the cover concrete fell away on the loaded side. **Figure 6** shows the relationship between the height up to which the cover

concrete was lost on the loaded side and shear-to-flexural capacity ratio. Here, we discuss specimens that failed in flexure and with an axial reinforcement ratio of over 3%. The height up to which the cover concrete was lost is divided by effective depth d in order to obtain non-dimensional index. When there is no gap between the lateral external reinforcement and the column surface, there was little difference in terms of loss of cover concrete between retrofitted specimens and RC specimens. However, when a gap is present, the cover concrete fell away up to a greater height than with RC specimens. This is because the external lateral reinforcement does not restrain buckling of the axial reinforcement and cracking of the cover concrete. But as shown in **Picture 1**, even in the case of RB-IV-1 which has some gap between lateral reinforcement and the column surface, severe damage on the shear resisting side was limited to about d , the effective depth. This is about the same as for specimens with no gap between the external reinforcement and the column surface as well as for normal RC specimens.



Picture 1 Damage condition of RB-IV-1

3.3 Strain of retrofitting bars and hoop reinforcement

Figures 7, 8, and 9 show measured strain values for the retrofitted bars in RB-III-1, -2, and -3. The figures show strain for the retrofitted bars at the front and the side of the specimen. The strain gages were fitted at the center of the retrofitted bars. The values used in these figures are the maximum values obtained during the loading cycle. In the case of RB-III-1, which has the highest ratio of retrofitted bars, the retrofitted bars on the front yielded at cycle 9 δy_{test} , and at the final stage, retrofitted bars in the range $0.5 d$ to $1 d$ (d : effective depth) yielded. On the other hand, on the side, no retrofitted bars yielded until the ultimate state, and only the lowest bar had yielded by the end of the test. In RB-III-2 (**Figure 8**), retrofitted bars 200 mm above the footing yielded at the same time on both the front and the side. The lowest bar also yielded on the

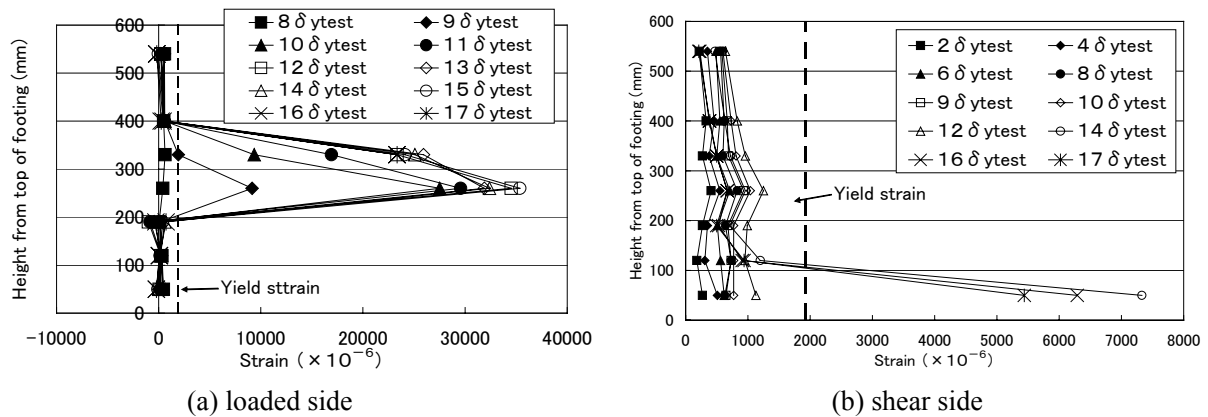
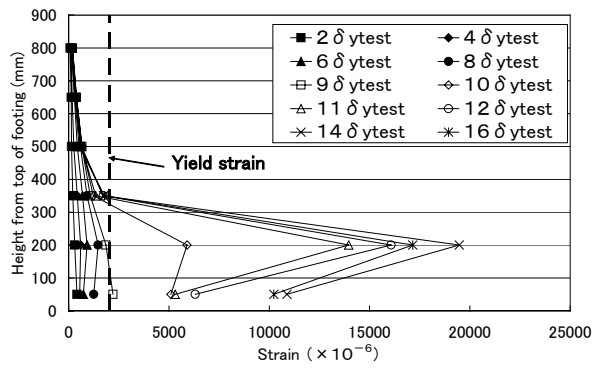
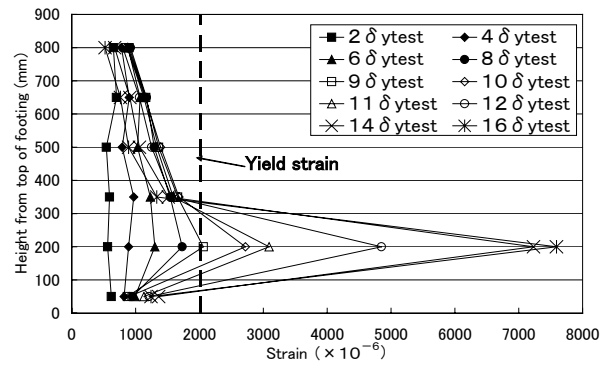


Figure 7 Measured values of retrofitted bar strain for RB-III-1

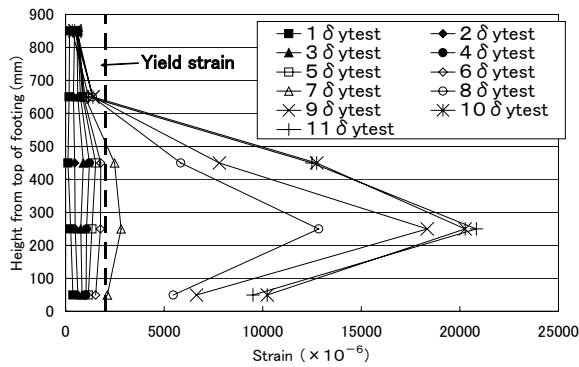


(a) loaded side

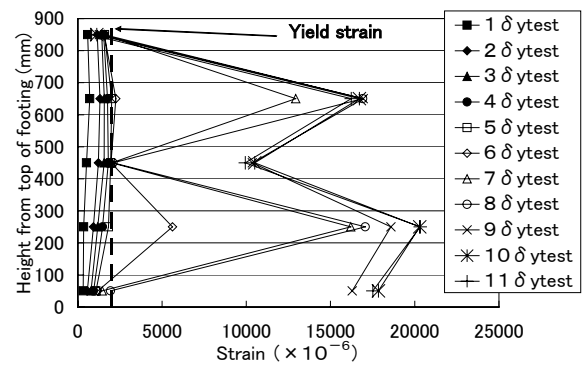


(b) shear side

Figure 8 Measured value of retrofitting bar strain for RB-III-2



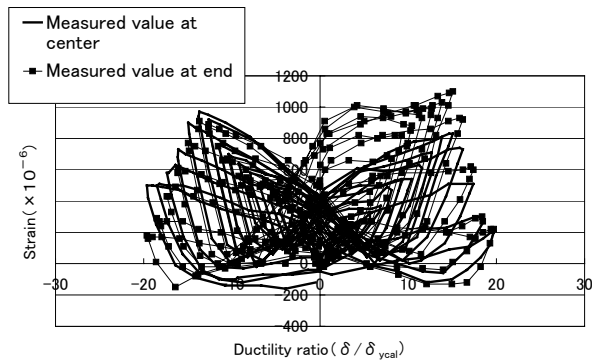
(a) loaded side



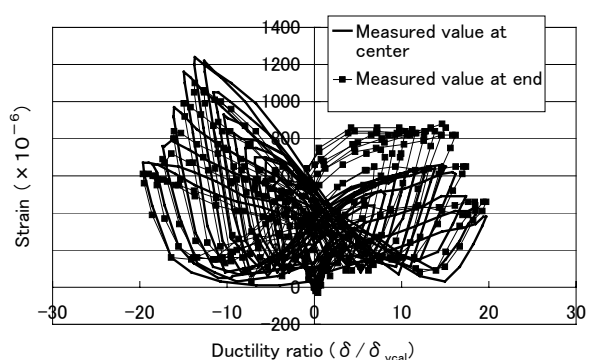
(b) shear side

Figure 9 Measured value of retrofitting bar strain for RB-III-3

front. In RB-III-3, which failed in shear after flexural yielding (**Figure 9**), retrofitted bars yielded at almost the same time on both the front and the side. The range of yielding was greater on the side. It was found that in the RB-III series, in which the retrofitted bars touch the surface of the column, the timing and range of initial cover concrete spalling almost coincided with yielding of the retrofitted re-bars on the front. Based on these results, we deduce that the retrofitted external reinforcement yielded as a consequence of axial reinforcement buckling [1].



(a) at height of 180 mm from footing



(b) at height of 245 mm from footing

Figure 10 Measured value of strain of strain of retrofitting bar of RB-III-1

Figure 10 shows measured values of retrofitted bar strain at heights 180 mm and 245 mm from the footing on the side. In this figure, measured values for both end and center of the same retrofitted bar are shown.

These values are almost same, so it can be said that strain is almost uniform from end to center when the retrofitted bars are in contact with the surface of the column.

Figures 11 and 12 show the measured values for RB-IV-1 and -2, in which the retrofitted bars do not touch the surface of the column. In the case of RB-IV-1 (**Figure 11**), bars on the front yielded at a height of 200 mm above the footing. This situation is the same as for RB-III-2, where the parameters are the same except for the gap between the retrofitted bars and the column surface. On the side, the maximum strain occurred in the range from 0.5 d to 1.0 d. Its value was about 75% of the yield strain, and the bars did not yield. With RB-IV-2 as shown in Figure 12, which failed in shear after flexural yielding, retrofitted bars on the front yielded in the range up to 250 mm (0.5 d) above the footing. This yielded range is less than that of RB-III-3, which has almost the same parameters as RB-IV-2 except for the gap between the retrofitted bars and the column surface. At a height of 250 mm on the side, the retrofitted bar strain was close to the yield strain. However, these retrofitted bars on the lateral part did not yield.

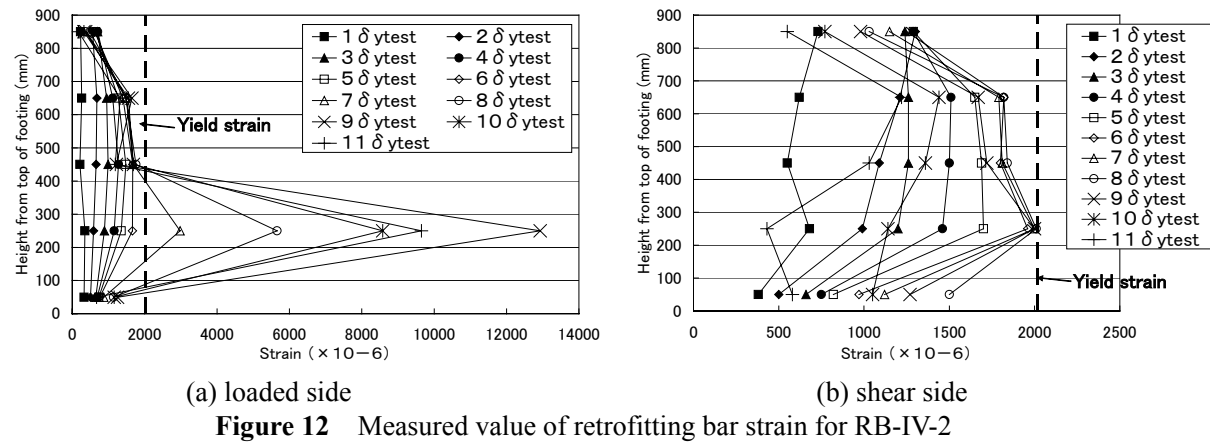
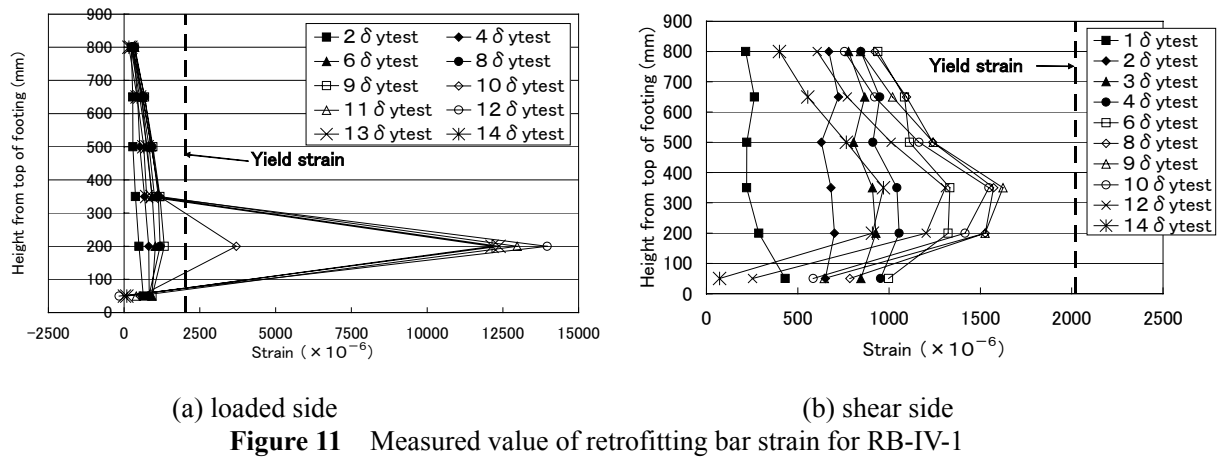
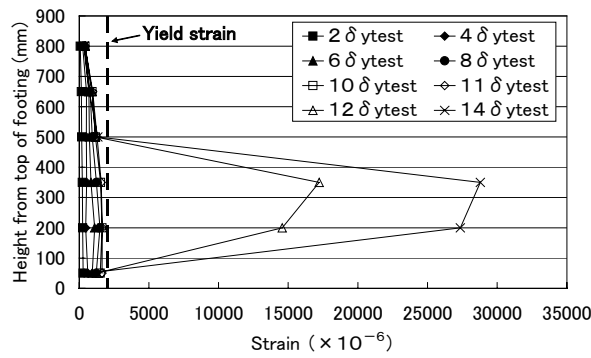
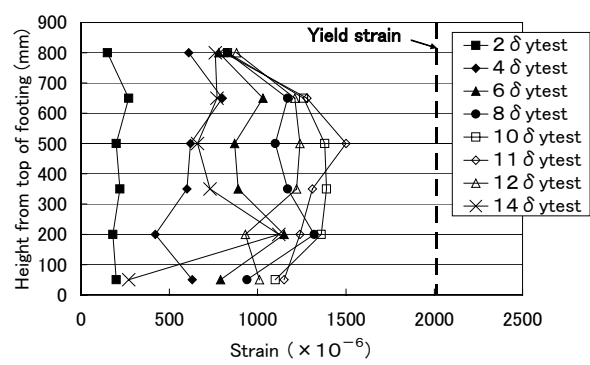


Figure 13 shows the experimental values for RB-V-3, in which the anchors are separate and the retrofitted bars do not touch the column. On the front, the retrofitted bars at heights 200 mm and 350 mm above the footing yielded. The yielding range was greater than that of RB-IV-1. On the side, the retrofitted bar strain was about 75% of the yield strain. These results are similar to those for RB-IV-1, so, it can be calculated that separation anchors have little influence on structural performance of the column.

Figure 14 and 15 show the experimental results for RB-VI-1 and RB-VI-2, which have a large section. In the case of RB-VI-1, retrofitting bars up to 300 mm (0.55 d) above the footing yielded on both the front and the side, as shown in **Figure 14**. This yield range was almost equal to that of RB-III-2, which has almost the

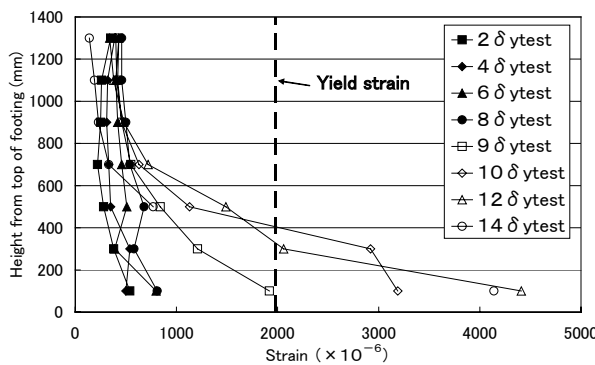


(a) loaded side

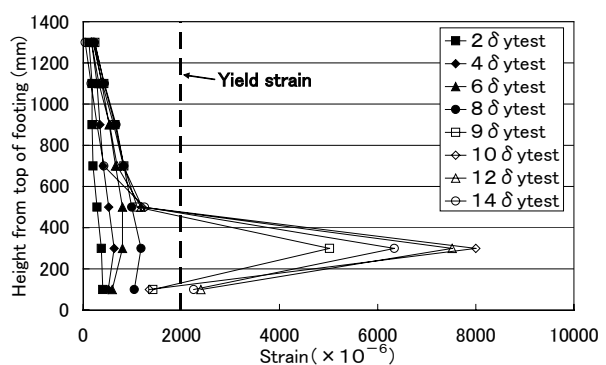


(b) shear side

Figure 13 Measured value of retrofitting bar strain for RB-V-3

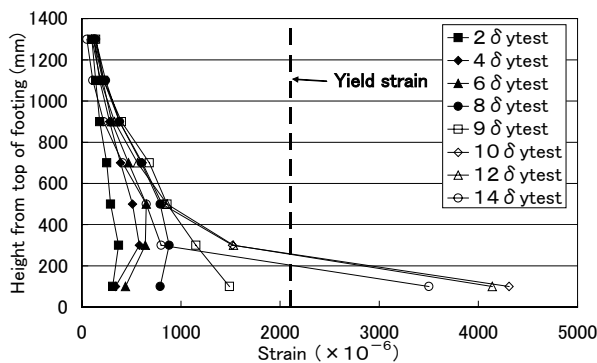


(a) loaded side

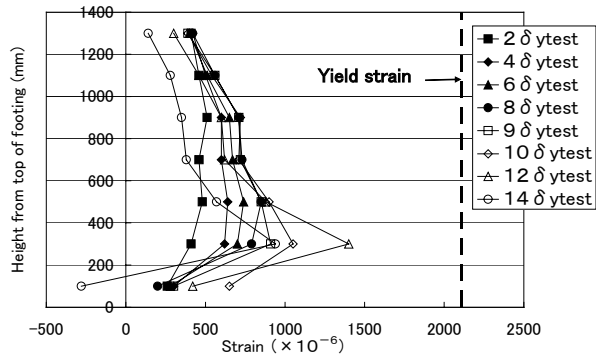


(b) shear side

Figure 14 Measured value of retrofitting bar strain for RB-VI-1



(a) loaded side

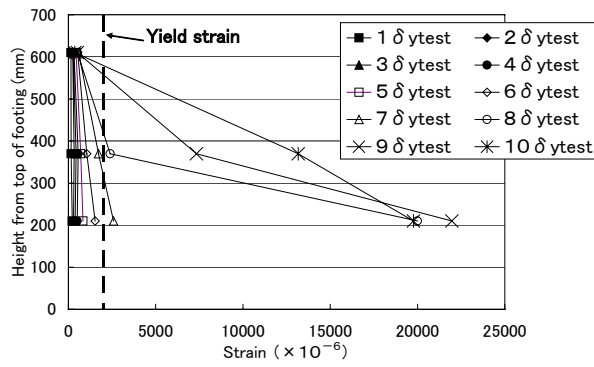


(b) shear side

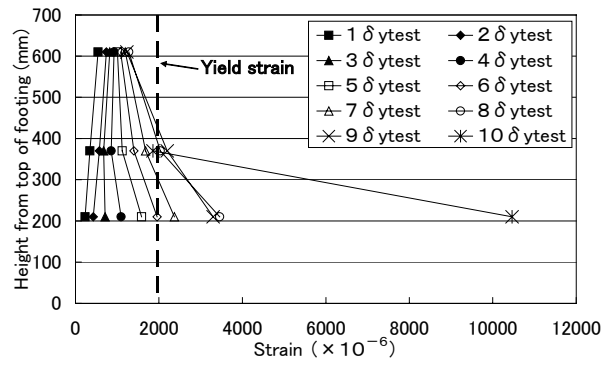
Figure 15 Measured value of retrofitting bar strain for RB-VI-2

same parameters except section size. With RB-VI-2, only the lowest bars yielded on the front, while on the side the maximum strain of retrofitted bars was less than 70% of the yield strain.

In summary, when a column is retrofitted, retrofitted bar strains are greatly affected by their quantity and by the gap between retrofitted bars and the column surface. For example, in cases RB-III-1 ($V_{yd}/V_{mu}=2.38$) and RB-VI-2 ($V_{yd}/V_{mu}=2.27$), retrofitted bars on the front yielded, but bars on the side did not yield. In the case of RB-III-3 ($V_{yd}/V_{mu}=1.42$), RB-IV-1 ($V_{yd}/V_{mu}=1.41$), RB-V-3 ($V_{yd}/V_{mu}=1.50$), and RB-VI-1 ($V_{yd}/V_{mu}=1.52$), bars on the front yielded. On the other hand, on the side, retrofitted bars yielded in cases where they were in contact with the column surface, while they did not when there was no contact. In cases

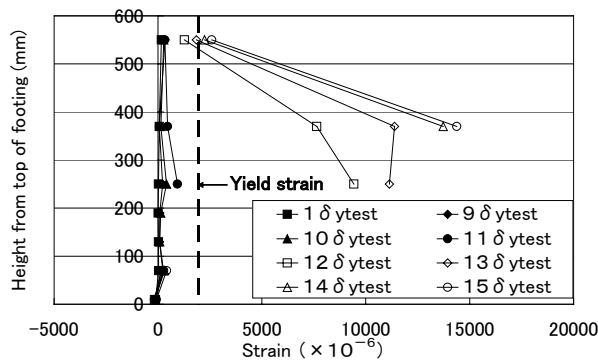


(a) loaded side

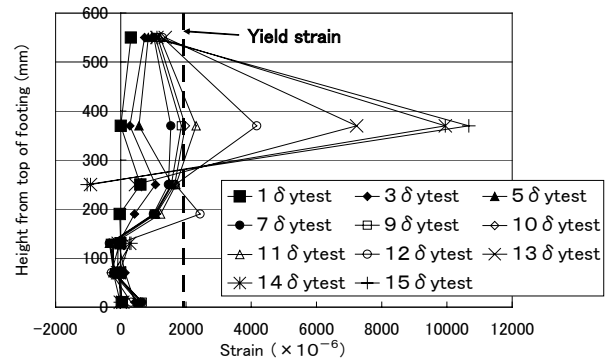


(b) shear side

Figure 16 Measured value of hoop reinforcement strain for RC-A1

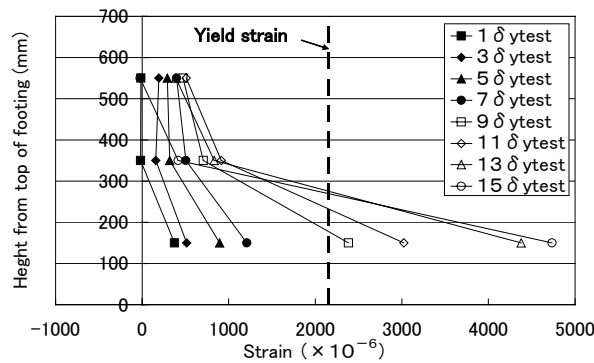


(a) loaded side

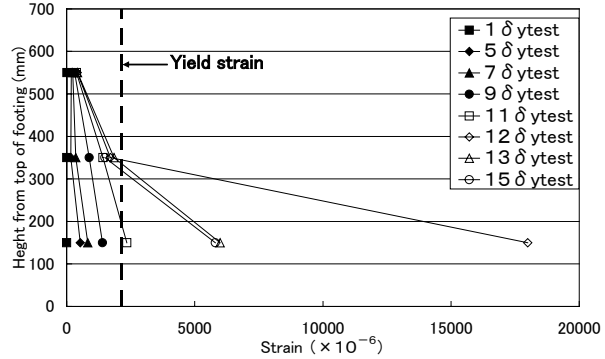


(b) shear side

Figure 17 Measured value of hoop reinforcement strain for RC-No.6



(a) loaded side



(b) shear side

Figure 18 Measured value of hoop reinforcement strain for RC-A9

RB-III-3 and RB-IV-2, which failed in shear after flexural yielding, bars on the front yielded. However, bars did not yield. In this case, the retrofitted bars did not touch the column surface.

Figures 16, 17, and 18 show experimental strain values of hoop reinforcement in ordinary RC columns. In RC-A1, the hoop reinforcement yielded at the same time on the front and side as shown in **Figure 16**. The range over which yielding occurred was about 0.5 to 1.0 d from the top of the footing, and this was almost the same on both the front and the side. **Figure 17** shows the experimental results for RC-No.6. In this case, the hoop reinforcement yielded first on the side. The range of yielding was about 0.5 to 1.5 d from the footing on the front, and 0.5 to 1.0 d on the side. **Figure 18** shows the experimental results for RC-A9. Hoop

reinforcement yielded at the same time on the front and the side. The range of yielding was also almost the same.

To summarize the discussion above, in the case of RC columns with a shear-to-flexural capacity ratio of 2.0 to 3.0, hoop reinforcement yielded in all specimens, and the range of yielding above the footing was almost the same. In the case of retrofitted specimens with a shear-to-flexural capacity ratio of over 2.0, retrofitted bars on the side did not yield. This contrasts with the case of RC specimens, in which hoop reinforcement on the side yielded even when shear-to-flexural capacity ratio was over 2.0.

3.4 Shear force supported by retrofitted bars and hoop reinforcement

Figures 19 and 20 show the shear force and V_s' in the case of RB-III-1 and RC-No.6, both of which have a shear-to-flexural capacity ratio of about 2.5. Here, V_s' is the calculated shear force as based on truss theory using measured values of retrofitted bar strain and hoop reinforcement strain. In **Figures 19 and 20**, the horizontal axis is the ductility ratio (δ/δ_{ycal} ; δ : horizontal deformation; δ_{ycal} : calculated value of yield deformation), the left vertical axis is load (kN), and the right axis is f_w/f_{wy} (f_w : calculated stress using measured strain values of retrofitted bars and hoop reinforcement; f_{wy} : yield strength of retrofitted bars and hoop reinforcement). f_w/f_{wy} was fixed at 1.0 after yielding. The values used for calculation were measured 350 mm above the top of the footing, because the main shear crack intersected retrofitted bars and hoop reinforcement at this height. As deformation becomes more severe, V_s' gradually increases. This is because V_c (V_c : ultimate shear strength without shear reinforcement) gradually falls during cyclic loading. The V_s' values shown in **Figures 19 and 20** are calculated values based on truss theory using the raw measured strain values of retrofitted bars and hoop reinforcement. Consequently, these values certainly include the influence of deformation toward the outside caused by buckling of the axial reinforcement on the loaded side, and do not indicate the real shear force supported by the steel bars. However, when the ductility ratio (δ/δ_{ycal}) is less than 5, the influence of buckling is thought to be very small. In this range, the rate of increase of V_s' is grater in the case of RC columns than in the case of retrofitted columns. This indicates that the fall in V_c of an RC column during cyclic loading is larger than that of a retrofitted column. As can be seen in **Figure 20**, V_s' exceeds the actual shear force in the case of RC-No.6. This may be because V_s' includes the influence of axial reinforcement buckling as mentioned above.

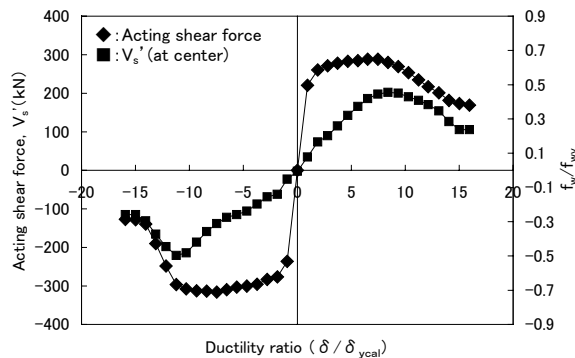


Figure 19 Acting shear force and V_s' for RB-III-1

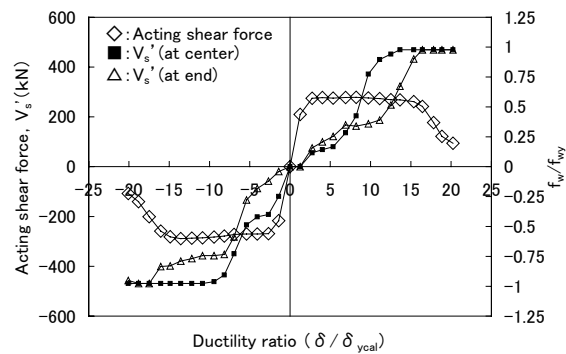


Figure 20 Acting shear force and V_s' for RC-No.6

Kinugasa et al [5] indicated that failure of the core concrete during cyclic loading results from softening of the aggregate interlocking action or diagonal cracking. In our experiments, it is possible that the influence of shear reinforcement bonding on softening of aggregate interlocking is being observed. In other words, in the case of ordinary RC columns with hoop reinforcement inside the section, the hoop reinforcement strain is not uniform and becomes extremely large at the crack. As a result, residual strain after unloading is high, which prevents closing of the cracks. A remarkable decrease in V_c is the result. On the other hand, in the case of retrofitted columns with external lateral reinforcing bars, the retrofitted bar strain is not localized at the crack position. Therefore, the decrease in V_c due to cyclic loading may be small.

As shown in **Figure 7**, the hoop reinforcement strain at a point 330 mm above the top of the footing on the compressive side in RB-III-1 reached the yield at 9 δ test loading. After that, the strain increased due to push-out of the hoop reinforcement caused by buckling of the axial reinforcement. But, as shown in **Figure 19**, the influence of axial reinforcement buckling on the side seem small, and as the horizontal force decreases, the retrofitted bar strain also decreases. The maximum f_w/f_{wy} at a height of 330 mm was about 50%. In the case of RC-No.6, the hoop reinforcement yielded at 12 δ test loading on the compressive side in **Figure 17**. In **Figure 20**, the measured values at the end of hoop reinforcement are larger after the horizontal loading falls and yielding ultimately occurs there. This may be because the hoop reinforcement is pushed out of the compressive side by buckling of the axial reinforcement.

Figures 21 and 22 show the acting shear force and V_s' for RB-III-2 and RB-IV-1, which have a shear-to-flexural capacity ratio of about 1.4. In the case of RB-III-2, retrofitted bars on the side yielded, while they did not yield in the case of RB-IV-1. The strain values were measured at height of 200 mm above the top of the footing, the height at which the maximum value was obtained. Compared with RC-No.6 in **Figure 20**, the rate of increase of f_w/f_{wy} is smaller in the case of retrofitted columns. When retrofitted bars yielded, as in case RB-III-2, the loss of V_c becomes small.

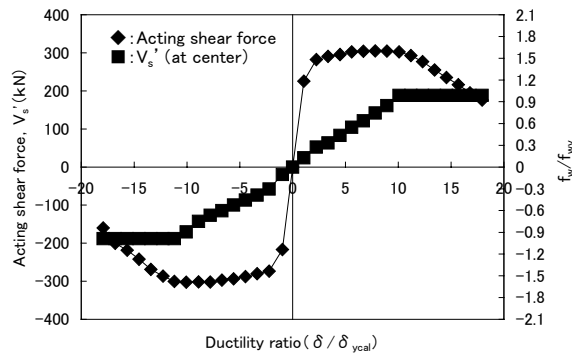


Figure 21 Acting shear force and V_s' for RB-III-2

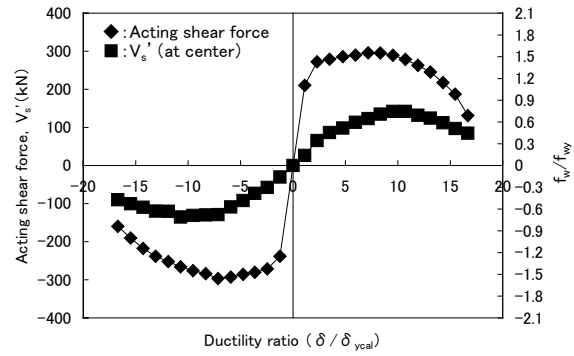


Figure 22 Acting shear force and V_s' for RB-IV-1

Figure 23 shows the relationship between f_w/f_{wy} and V_{yd}/V_{mu} for the retrofitted columns. These are the maximum values of f_w/f_{wy} for each specimen. f_w/f_{wy} was 0.8 to 0.9 for shear-to-flexural capacity ratios of about 1.4 when the retrofitting bars were in contact with the column surface. On the other hand, f_w/f_{wy} was about 0.75 when the shear-to-flexural capacity ratio was about 2.3 and the retrofitting bars were in contact with the column surface.

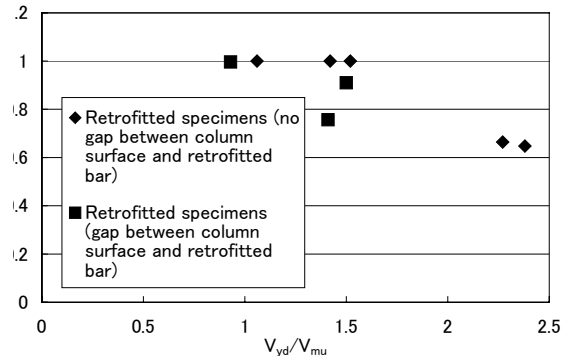


Figure 23 Relationship between f_w/f_{wy} and V_{yd}/V_{mu} for retrofitted columns

3.5 Deformability

Figure 24 shows the relationship of ductility ratio to V_{yd}/V_{mu} for all specimens indicated in **Table 1**. Data for RC additional specimens that failed in shear after yielding are also included. These additional specimens were loaded differently with three cycles at each loading deformation. In **Figure 24**, retrofitted columns with lateral external reinforcing bars have greater ductility than ordinary RC columns for similar V_{yd}/V_{mu} . In particular, the retrofitted specimen with a shear-to-flexural capacity ratio of 1.4 has almost the same deformability as the RC specimen with a shear-to-flexural capacity ratio of over 2.0. This is because retrofitted bar strain is not localized at the crack position, as mentioned earlier in this discussion. This is also considered one of the reasons for the minimal influence push-out from the compressive side as a result of axial reinforcement buckling.

4. CONCLUSION

The following conclusions can be drawn from the experimental results and discussions presented here:

(1) When column specimens fail in flexure, the height range over which cover concrete spalling occurred on the compressive side and the range of major core concrete damage was about 1 d from the footing. Similar failure conditions were observed both for retrofitted columns and ordinary RC columns. However, the range of cover concrete spalling increased to 1.5 d in the case of retrofitted specimens where the retrofitted bars did not touch the column surface.

(2) In retrofitted specimens whose shear-to-flexural capacity ratio was over 1.0, the retrofitted bars did not yield when they were out of contact with the column surface. Retrofitted bars did not yield when shear-to-flexural capacity ratio was over 2.4 and retrofitted bars were contact with the column surface. When specimens failed in flexure and the retrofitted bars did not yield on the side, the maximum retrofitted bar strain on the side was 75% to 90% of the yield strain.

(3) Specimens retrofitted with lateral external reinforcing bars have greater deformability than ordinary RC specimens as long as bond failure of the axial reinforcement does not occur.

(4) The decrease in V_c during cyclic loading may be smaller in retrofitted specimens than in ordinary RC specimens. In RC columns, the hoop reinforcement strain is localized and extremely large at the crack section, and residual strain after unloading is high. As a result, the hoop reinforcement prevents closing of the crack, thus damaging the core concrete. This is the cause of the large fall in V_c .

Acknowledgements; We thank Prof. Maekawa (University of Tokyo) for his kind and valuable advices during this work.

References

- [1] Tsuyoshi, T., Ishibashi, T., Kobayashi, M., and Tatsuki, T., "An Experimental Study on Seismic Retrofitting Methods for Existing Reinforced Concrete Columns with External Lateral Reinforcement Anchored at Four Corners of Columns", Proceedings of JSCE, No.662/V-49, pp.205-216, November 2000 (in Japanese)
- [2] East Japan Railway Company, Guidelines for RB method, March 2000 (in Japanese)
- [3] Ishibashi, T., Tsuyoshi, T., Kobayashi, K., and Kobayashi, M., "An Experimental Study on Damage Levels and Repairing Effects of Reinforced Concrete Columns Subjected to Reversal Cyclic Loading with Large Deformations", Proceedings of JSCE, No.648/V-47, pp.55-69, May 2000 (in Japanese)
- [4] Railway Technical Research Institute, Standard specifications for design of concrete structures for railways, 1992 (in Japanese)
- [5] Kinugasa, H., and Takayanagi, M., "Failure Behavior of RC Columns Subjected to Cyclic Loading in Large Deformation Range under Low Axial Loading", Proceeding of JCI, Vo.22, No.3, pp.223-228, 2000

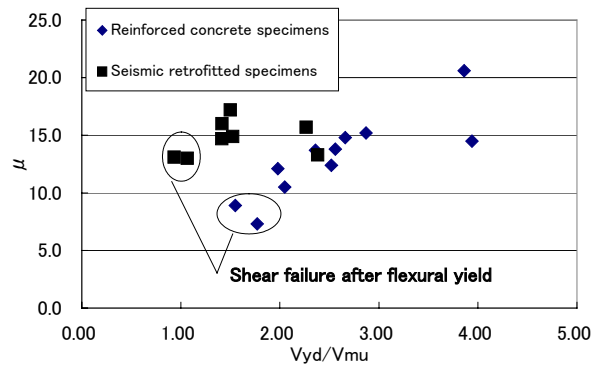


Figure 24 Relationship between ductility ratio and V_{yd}/V_{mu}